Chapter 5
Results and Discussion

5.1 Introduction to and Notes on Results

In this work, we are interested in the particle flux/(time · area · solid angle · kinetic energy/nucleon), j, which is observable; in particular, we are interested in the shape of $\langle j \rangle_\mu$ vs. z and the spectral index, γ, which is used to indicate the acceleration efficiency at the momentum of interest.

As discussed in §2.1.2, the spectral index, γ, is a power-law index over momentum in the relation $j \propto p^{-\gamma}$. When we take logarithm of this relation, it yields $\log j = -\gamma \log p + \text{const}$. If we plot a graph of $\log j$ vs $\log p$, $-\gamma$ will be the slope of the graph. Therefore, we can define a local power-law index, γ, even if the large-scale behavior is not a single power law (even if γ is not constant with p).

If the γ value is low, j slowly decreases in p, which means the acceleration efficiency is high. On the other hand, if the γ value is large, j rapidly decreases in p, meaning the acceleration efficiency is low (see Figure 5.1). Note that, in this work, γ is based on $\langle j \rangle_\mu$ far downstream, denoted by $\langle j \rangle_1$, where 1 refers to the first z-step (z far downstream), because the overall particle population is dominated by the downstream population which is nearly constant in position.

Although the transport equations we use are not written in terms of j, the calculated F can be related to j. Because $F = 2\pi A j$, where A is the cross-sectional area perpendicular to z, and A is constant throughout the simulation

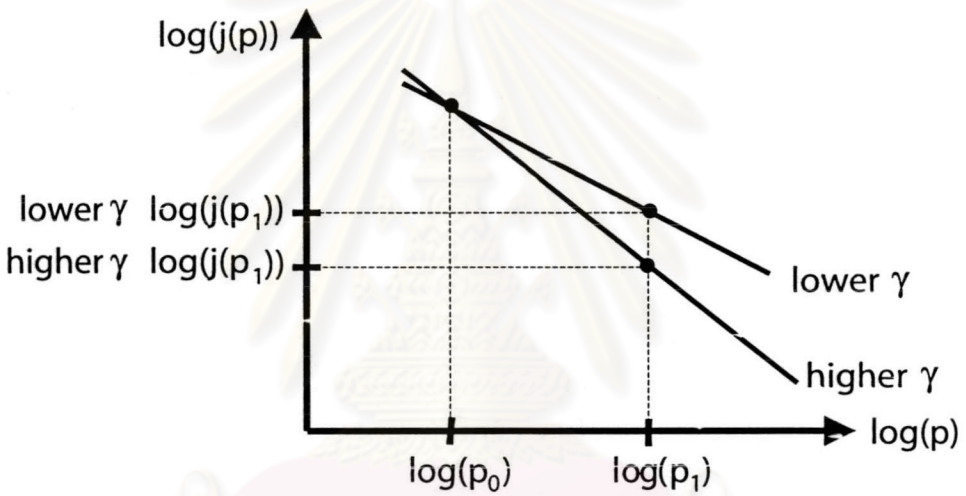

Figure 5.1: Two graphs of $\log j$ vs. $\log p$ with two different γ values: $-\gamma$ is the slope of the graph, used to indicate acceleration efficiency at the momentum of interest, p_0. For the same particle density at p_0, a higher γ at p_0 gives a smaller particle number density at a higher momentum, p_1; a lower γ at p_0 gives a greater particle number density at a higher momentum, p_1. Therefore, a lower γ implies a greater acceleration efficiency.

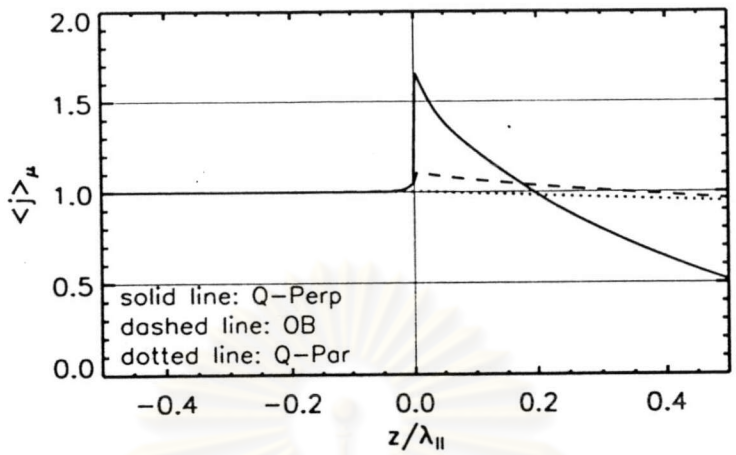

Figure 5.2: Steady state spatial density of particles with an energy corresponding with $v/U_{1n} = 25$ in the cases of shocks, obtained from solving the pitch-angle transport equation. The jump height is highest in the quasi-perpendicular case (Q-Perp; solid line), lower in the oblique case (OB; dashed line), and disappears in the quasi-parallel case (Q-Par; dotted line).

region, the shape of $\langle j \rangle_\mu$ vs. z and $\langle F \rangle_\mu$ vs. z are just scaled differently. Moreover, the slopes of $\log\langle j \rangle_\mu$ vs. $\log p$ and $\log\langle F \rangle_\mu$ vs. $\log p$ are exactly the same.

Selected results are shown in this chapter, and all results are shown in Appendix D.

5.2 Results and Discussion

In the cases of shocks, our pitch-angle transport simulation results show a jump in particle density from downstream to upstream (see also Ruffolo 1999, Gieseler et al. 1999). Moreover, we verified that the jump height depends on the field angle. The jump is highest in the case of a quasi-perpendicular magnetic field. It is lower in the case of an oblique magnetic field, and in the case of a quasi-parallel magnetic field, the jump disappears (see Figure 5.2).

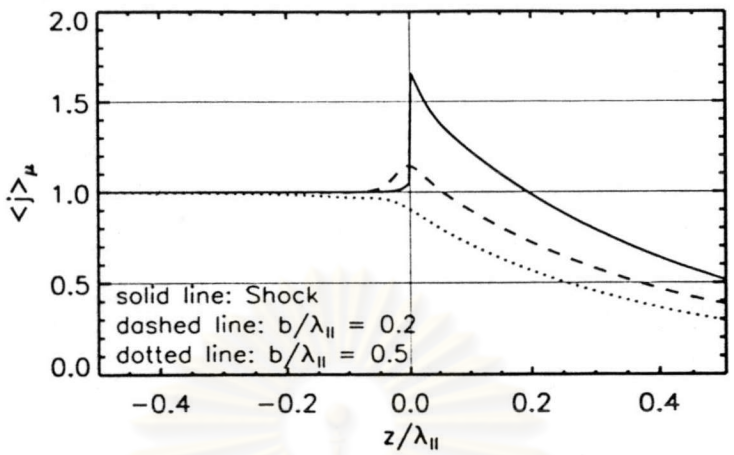

Figure 5.3: Steady state spatial density of particles with an energy corresponding with $v/U_{1n} = 25$ in the cases of a quasi-perpendicular shock (solid line), compression region with $b/\lambda_{\|} = 0.2$ (dashed line), and compression region with $b/\lambda_{\|} = 0.5$ (dotted line), obtained from solving the pitch-angle transport equation

In the cases of narrow compression regions, the results from pitch-angle transport give a peak at the center of the compression. The peak height is not as high as the jump height for the corresponding shock, and the peak height decreases when the compression becomes wider (see Figure 5.3). However, the peak can only be found in the results from pitch-angle transport equation. The approximate diffusion-convection equation does not yield a peak in any cases (see Figure 5.4).

The reason is because the systematic changes in pitch angle, and in particular the "mirroring effect," are taken into account only by pitch-angle transport, while they are not in the diffusion-convection (or diffusion-convection-acceleration) approach. In addition, the peak (and jump) height is stronger when shocks/compressions are more perpendicular, and compressions are narrower, which is consistent with a dependence on the strength of the magnetic

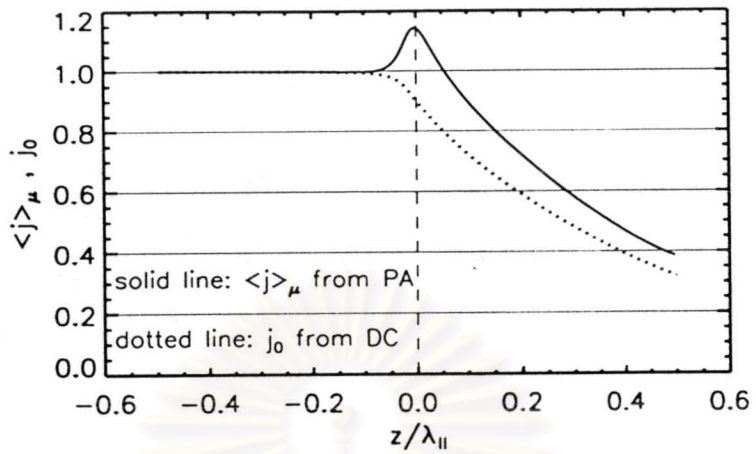

Figure 5.4: Steady state spatial density of particles with an energy corresponding with $v/U_{1n} = 25$ in the case of a quasi-parallel compression region with $b/\lambda_{\|} = 0.2$, obtained from solving the pitch-angle transport equation (PA; solid line) and diffusion-convection equation (DC; dotted line).

mirroring effect. Therefore, we call this the "mirroring peak."

Regarding the particle spectrum, pitch angle transport does not yield the exact power-law spectrum in cases of shocks as predicted by the diffusion-convection equation; slopes of spectra in a log-log scale, $-\gamma$, depend on particle momentum, especially in the case of a quasi-perpendicular magnetic field (see Figure 5.5). Moreover, from the results for cases of shocks and narrow compressions we found that the γ value, indicating the acceleration efficiency, is associated with the mirroring peak in the spatial distribution of particles. The pitch-angle transport equation yields a harder spectrum (lower γ: greater acceleration efficiency) than predicted by the diffusion-convection equation. The difference between γ from the pitch-angle transport equation and γ from the diffusion-convection equation is greater when shocks/compressions are more perpendicular and compressions are narrower, corresponding with the mirroring peak height (see Figures

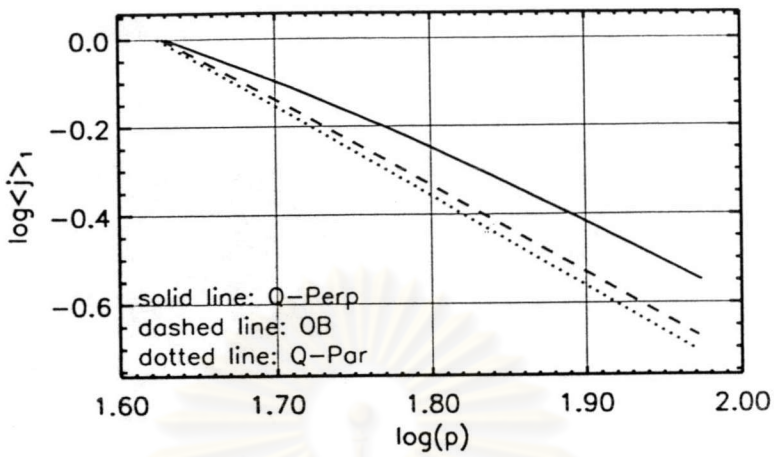

Figure 5.5: Particle spectra of quasi-perpendicular (Q-Perp; solid line), oblique (OB; dashed line) and quasi-parallel (Q-Par; dotted line) shocks, obtained by the pitch-angle transport equation. Here, they are normalized to one at the momentum corresponding with $v/U_{1n} = 25$.

5.6 and 5.7). For this reason, it can be concluded that the mirroring effect also contributes to increased efficiency of particle acceleration.

Additionally, as shown in Figures 5.6 and 5.7, a difference between pitch-angle transport and diffusion-convection results is also found for cases of wide compressions. This is not an effect of magnetic mirroring because the difference is clearer when the compressions are wider (weaker mirroring effect). Actually, it is a consequence of the assumption $j(z,p) \propto p^{-\gamma}$ in the diffusion-convection approach. The assumption implies that the z-dependence of $j(z,p)$ has to be independent of p throughout the acceleration region, but in fact it is not. In Figure 5.8, it is evident that the normalized spatial density (j far downstream is normalized to be 1) for a lower energy is not the same as for a higher energy. At a lower energy there is a smaller particle density at the compression center, which has the highest acceleration rate. Then, under the diffusion-convection

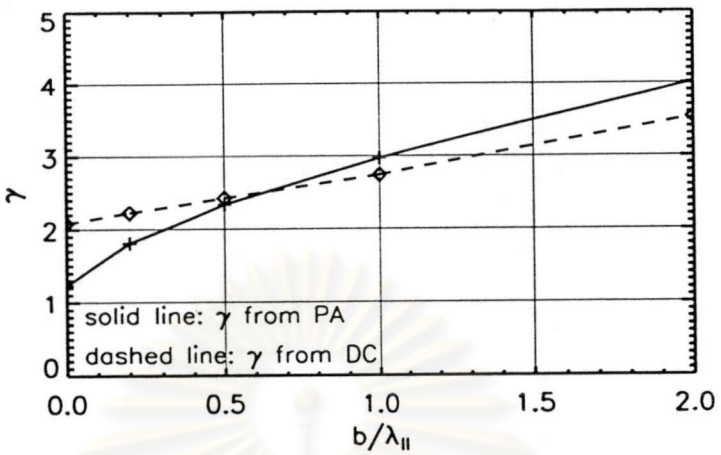

Figure 5.6: Spectral index, γ, of particles with an energy corresponding with $v/U_{1n} = 25$ versus width of compression (shock $\equiv$ zero width compression region) in the cases of quasi-perpendicular shock/compression regions, obtained from solving the pitch-angle transport equation (PA; solid line) and diffusion-convection equation (DC; dotted line).

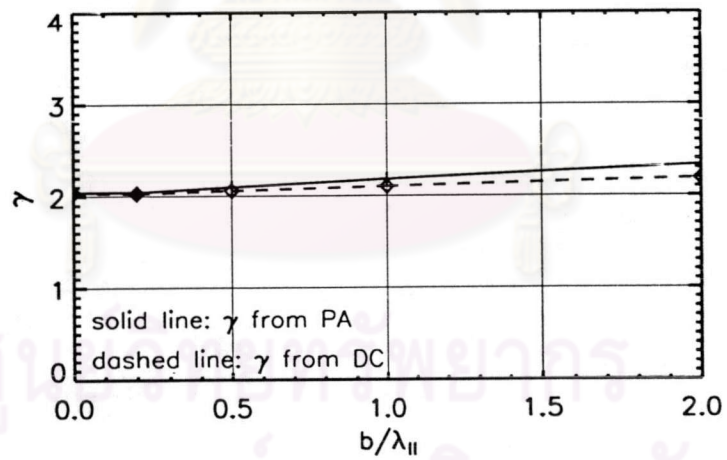

Figure 5.7: Spectral index, γ, of particles with an energy corresponding with $v/U_{1n} = 25$ versus width of compression (shock $\equiv$ zero width compression region) in the cases of quasi-parallel shock/compression regions, obtained from solving the pitch-angle transport equation (PA; solid line) and diffusion-convection equation (DC; dotted line).

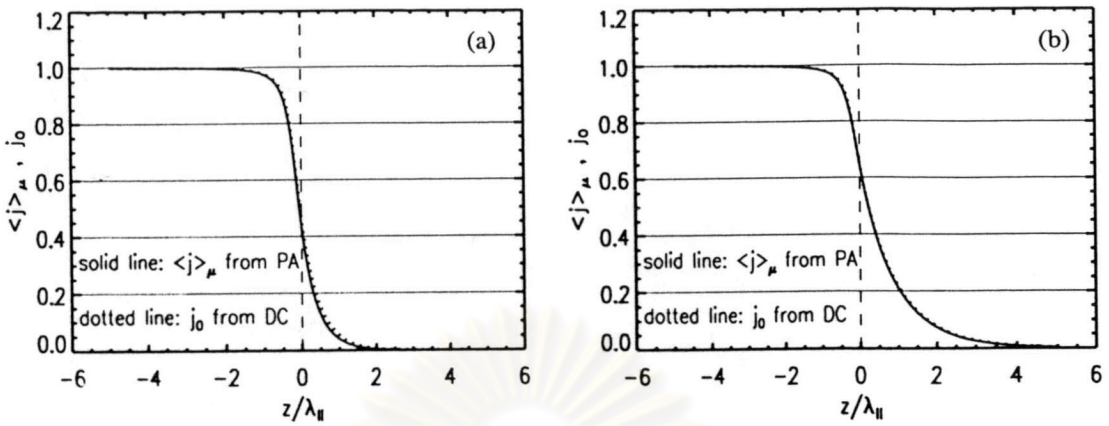

Figure 5.8: Steady state spatial density of particles with an energy corresponding with (a) $v/U_{1n} = 25$ and (b) $v/U_{1n} = 50$ in the case of a quasi-perpendicular compression region with $b/\lambda_{\parallel} = 2.0$, obtained from solving the pitch-angle transport equation (PA; solid line) and diffusion-convection equation (DC; dotted line).

assumption, the particles will be accelerated from lower energies to an energy of interest more than they should be; i.e., γ will be lower than it should be. In cases where the spatial distribution at different energies is not very different at the compression center, the diffusion-convection equation will predict a γ value that is not much lower than it should be (see Figure 5.9).

Although the diffusion-convection equation might give incorrect results for the momentum distribution and spectral index, it still yields reasonable spatial distributions when the magnetic mirroring effect is weak (see Figures 5.8 and 5.9).

Notwithstanding, both spatial distribution and spectrum differences obtained by the pitch-angle transport and diffusion-convection equations will be smaller when the particle momentum, or more precisely, v/U_{1n}, becomes greater. Referring to Figure 5.5, at least for the clearly eye-catching quasi-perpendicular case, the spectrum is quite not a power law at low momenta and it has more power-law characteristics at higher momenta. Furthermore, Figures 5.4, 5.6, and

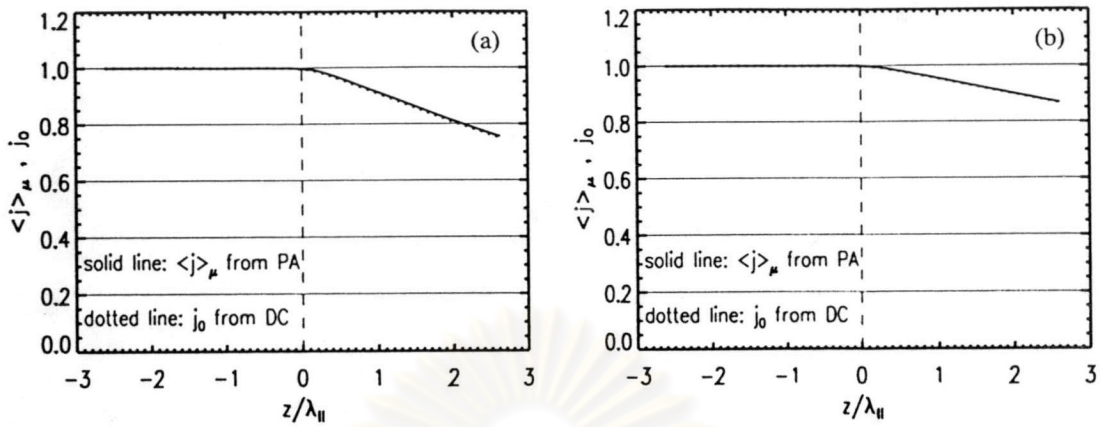

Figure 5.9: Steady state spatial density of particles with an energy corresponding with (a) $v/U_{1n} = 25$ and (b) $v/U_{1n} = 50$ in the case of a quasi-parallel compression region with $b/\lambda_{\parallel} = 0.2$, obtained from solving the pitch-angle transport equation (PA; solid line) and diffusion-convection equation (DC; dotted line).

5.7 can be respectively compared with Figures 5.10, 5.11, and 5.12 to indicate the small differences at a high momentum.

That means that for low energy particles, including the majority of solar energetic particles, using the pitch-angle transport equation is necessary to obtain an appropriate spatial distribution and spectrum of particles, especially in cases of high magnetic mirroring.

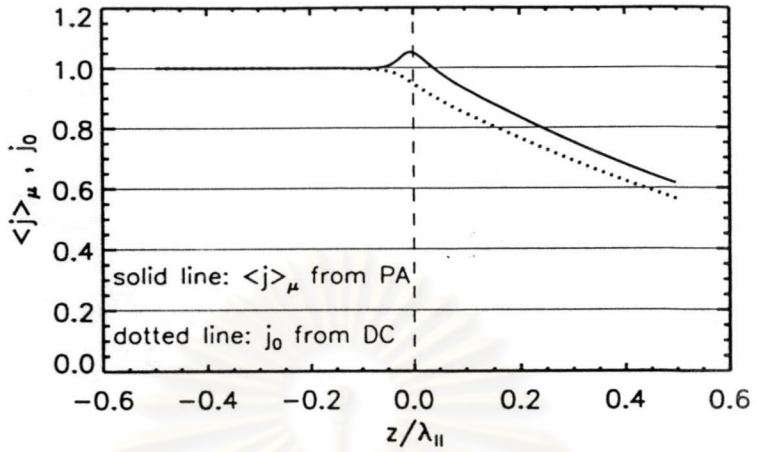

Figure 5.10: Steady state spatial density of particles with an energy corresponding with $v/U_{1n} = 50$ in the case of a quasi-parallel compression region with $b/\lambda_{\parallel} = 0.2$, obtained from solving the pitch-angle transport equation (PA; solid line) and diffusion-convection equation (DC; dotted line).

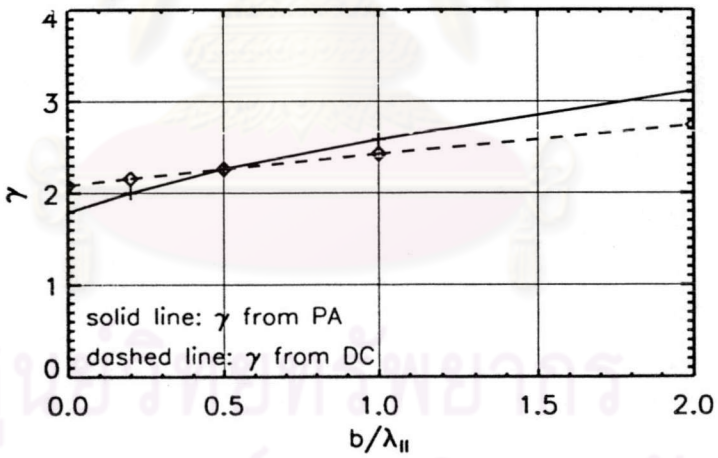

Figure 5.11: Spectral index, γ, of particles with an energy corresponding with $v/U_{1n} = 50$ versus width of compression (shock $\equiv$ zero width compression region) in the cases of quasi-perpendicular shock/compression regions, obtained from solving the pitch-angle transport equation (PA; solid line) and diffusion-convection equation (DC; dotted line).

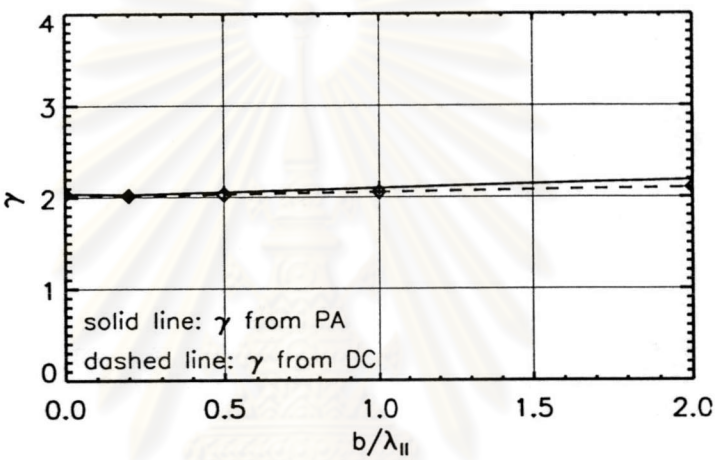

Figure 5.12: Spectral index, γ, of particles with an energy corresponding with $v/U_{1n} = 50$ versus width of compression (shock $\equiv$ zero width compression region) in the cases of quasi-parallel shock/compression regions, obtained from solving the pitch-angle transport equation (PA; solid line) and diffusion-convection equation (DC; dotted line).